Investigation of the Temporal Evolution of Translational Dynamics of Water Molecules in Hydrated Calcium Aluminate Pastes

Emiliano Fratini,[†,‡] Sow-Hsin Chen,[‡] and Piero Baglioni*[,†,‡]

Department of Chemistry and CSGI, University of Florence, via della Lastruccia 3 − Sesto Fiorentino, 50019 Florence, Italy, Department of Nuclear Engineering, 24-209, Massachusetts Institute of Technology, Cambridge, Massachusetts 02139

Received: January 8, 2003; In Final Form: May 23, 2003

We investigated the translational dynamics of water molecules in the hydrated aluminate and aluminum-ferrite pastes (C_3A and C_4AF), two main components of the Ordinary Portland Cement (OPC), using the incoherent quasi-elastic neutron scattering (QENS) technique. We used a high-resolution disk chopper spectrometer (DCS) at the Center For Neutron Research (NCNR) in NIST, with incident monochromatic neutrons of wavelength, $\lambda = 9$ Å, resulting in an energy resolution of 20 μeV, covering a Q-range from 0.31 to 1.22 Å^{-1}. QENS spectra have been analyzed with a translational "relaxing cage model" previously developed by us.[1] We were able to extract time evolution of three characteristic parameters of the setting pastes: p, β, and $\bar{\tau}$, describing the fraction of the bound water (p) and relaxation behavior of the glassy water (β and $\bar{\tau}$) present in the aluminate pastes during the last stage of the reaction kinetics. These parameters, obtained for the first time for C_3A and C_4AF, show striking difference from that obtained in previous experiments for calcium silicate pastes (C_2S and C_3S).[1,2]

Introduction

Ordinary Portland Cement (OPC) is one of the most used and important materials in construction and civil engineering industries. It is often referred to as a hydraulic material since it reacts with water to generate a hard, solid matrix that continues to increase in compressive strength even when it is placed in an excess of water. It is well established that common OPC powders are formed by four main components that contribute more than 90 wt % to the overall OPC composition, even though its composition varies according to the desired final application. These components are alite (Ca_3SiO_5, 50−70%), belite (Ca_2SiO_4, 20−30%), aluminate phase ($Ca_3Al_2O_6$, 5−15%), and celite ($Ca_4Al_2Fe_2O_{10}$, 5−15%).[3] The aluminate fraction, C_3A and C_4AF,[4] is mainly responsible for the short-time compressive strength and it is usually important in tuning the overall cement hydration characteristics since it can be used to shorten the cement induction time. Recently, we analyzed the hydration water dynamics during the hardening of C_3S and C_2S pure compounds by using the quasi-elastic neutron scattering technique.[1,2,5,6] It was shown that the setting process could be explained by invoking two main types of water inside a calcium silicate cement paste—an "immobile water" and a "glassy water". In fact, the water reacts with cement components being in part strongly bound to the hydration products and in part constrained in the resulting complex porous matrix.[1] This interpretation differs slightly from the classical approach[7,8] where the nonbounded water was considered completely free to move and its contribution to the total intensity was taken as Lorentzian.

It is worthwhile recalling that some NMR studies[9] consider more than the two different kinds of water used in our model. Water mobility based on T_1 and T_2 relaxation times cannot be directly compared to the translational motion of water molecule detected by the QENS experiment, since NMR mainly detects dipolar interactions mostly associated with rotational motion. The de-coupling of rotational and translational motions is not trivial in an NMR experiment,[10] particularly in a system subjected to a continuous change of chemical composition such as cement during the curing process.

The analysis of the elastic component of a spectrum permits determination of the temporal evolution of the fraction of water (the first type) that has reacted with the silicate matrix forming amorphous calcium silicate hydrate, C−S−H and crystalline Portlandite (CH). Free water was not detected just after 1 h from the beginning of the setting process, as demonstrated by the non-Lorentzian line shape of the quasi-elastic component of the QENS spectrum. The second type of water defined as "glassy water"and similar in dynamic behavior to a supercooled bulk water exhibits significant structural relaxation properties, and the intermediate scattering function (ISF) shows a slowly decaying component that can be accounted for by the stretch exponent $\beta < 1$. Water is glassy just after 1 h from the beginning of the curing process and becomes "glassier" as indicated by the monotonic decrease of the stretch exponent β with the aging of the C_3S and C_2S pastes. Moreover, the relaxation parameters of the unreacted water, β and $\bar{\tau}$, could be extracted from the quasi-elastic contribution of the spectra assuming the relaxing cage model[11] formulation, inspired by the Mode Coupling Theory of supercooled liquids.[12,13] These two parameters represent: the deviation from the Debye-like relaxation (β) and the average relaxation time for the "cage" surrounding a typical water molecule, $\bar{\tau}$. In this way, the confinement effect coming from the hardening of the cement matrix on the unreacted water is determined and gives a complete picture of the hydration reaction. The curing process appears as a continuous conversion of glassy water into immobile water. These results were fully confirmed by differential scanning calorimetry (DSC) studies where we proposed a new method to investigate the curing and hardening of pure cement pastes and in the presence of superplasticizers.[14,15]

Previous investigations are here extended to underline the differences on the hydration process between the reactions taking place inside different cement pastes. In fact, while the C_3S and

* Author to whom correspondence should be addressed. Voice: +39 055 457 3033. Fax: +39 055 457 3032. E-mail: piero.baglioni@unifi.it.
† University of Florence.
‡ Massachusetts Institute of Technology.

10.1021/jp0340461 CCC: $25.00
Published on Web 08/20/2003

C_2S calcium silicates react slowly (days or months), the hydration product (C−S−H) is mainly amorphous[16] and only the secondary product (CH) presents crystalline features, aluminate phases react rapidly with water to form mostly crystalline hydration products. As a simple approximation, the final product of C_3A may be assumed to be the stable C_3AH_6 and the reaction may be represented by the equation: $C_3A + 6H \rightarrow C_3AH_6$.[17] This product has a cubic symmetry and usually comes from the rearrangement of more complex hydrates (C_4AH_{13} and C_2AH_8) formed as platelets with hexagonal symmetry, a morphology that resembles that of portlandite.[18] The hydration products formed by the ferrite solid solution, C_4AF, are usually described as being similar to those formed by C_3A but with Fe^{3+} partly substituted for Al^{3+}.[18]

The hydration process of the two pure phases rich in aluminates, C_3A and C_4AF, and the effect of a superplasticizer that retards the calcium silicate hydration are reported, and compared to the previously investigated C_2S and C_3S, to have a complete picture of the cement hydration process.

Experimental Methods

The hydrated paste was prepared by mixing 1 g of bi-distilled water with 2 g of tri-calcium aluminate, or tetra-calcium alumino-ferrite, dry powder (C_3A or C_4AF) in order to obtain a 0.5 water/calcium aluminate mass ratio. Samples where placed in a 0.5 mm thick aluminum cell coated with Teflon.[1] The volume fraction of water in the samples was less than 0.60, making a film of H_2O of an effective thickness less than 0.30 mm. For this reason no multiple scattering correction was applied in further data analysis because this contribution was negligible under the adopted experimental conditions. The dry powders were obtained as a gift from CTG-Italcementi with a specific surface area (BLAINE) of 0.48 ± 0.05 m^2/g and 0.54 ± 0.05 m^2/g and a median diameter of 16.4 and 12.4 μm for C_3A and C_4AF, respectively.

The cement paste hydration (curing process) was followed at 25 °C by recording QENS spectra over a range of Q every hour for about 2 days. In the case of C_3A, the 0.5 wt % of the NSF superplasticizer (sodium salt of sulfonated naphthalene−formaldehyde polycondensate, obtained from CTG-Italcementi) has been added to the paste to monitor the effect on the hydration process.

The quasi-elastic neutron scattering experiments were carried out at NCNR, using the high-resolution disk chopper spectrometer DCS.[19,20] This is a general purpose TOF spectrometer. A schematic layout of the DCS is given in Figure 1. The incident monochromatic neutron wavelength was 9.0 Å (1.01 meV), which resulted in an over-all energy resolution (fwhm) of about 20 μeV. The sample cell was placed at 45° to the direction of the incident neutron beam. The detectors were grouped to obtain a set of five spectra in the Q range from 0.31 $Å^{-1}$ to 1.22 $Å^{-1}$. The data were corrected for scattering from the same sample holder containing dry calcium aluminate or alumino-ferrite powder and standardized by dividing by the scattering intensity from a thin vanadium plate (which gives the energy resolution function $R(\omega)$) and converted to the double differential scattering cross-section using standard routines available at NIST.

Results and Discussion

In previous papers[1,2] we showed that water dynamics in calcium silicate pastes can be described with a simple model where at a given time there are two categories of water molecules: a fraction p of immobile water molecules bound inside the hydration products, and a fraction $1 - p$ of glassy water

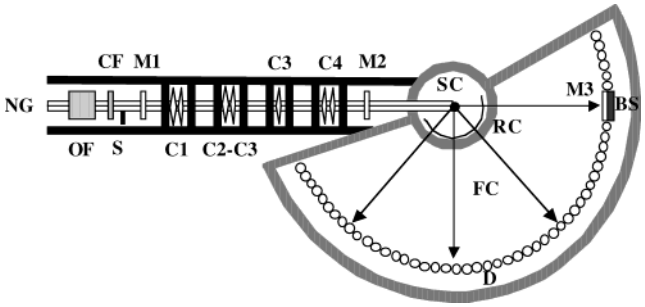

Figure 1. Schematic diagram of DCS high-resolution chopper time-of-flight (TOF) spectrometer. It is a general purpose direct geometry TOF spectrometer which uses seven synchronized disk choppers spinning at high speed (up to 20000 rpm) to produce a pulsed monoenergetic neutron beam. Energies of the scattered neutrons are measured by their individual TOF over a fixed distance of 4.01 m. Legend for the abbreviation from left to right: **NG** = Neutron Guide, **OF** = Optical Filter, **S** = Shutter, **CF** = Crystal Filter, **M1** = White Beam Monitor, **C1** = Pulsing Choppers, **C2** = Frame Overlap Chopper, **C3** = Order Removal Choppers, **C4** = Monochromatic Choppers, **M2** = Monochromatic Beam Monitor, **SC** = Sample Chamber, **FC** = Argon-Filled Flight Chamber, **RC** = Radial Collimator, **D** = ^{3}He Detectors, **M3** = Transmitted Beam Monitor, **BS** = Beam Stop.

molecules imbedded in the amorphous gel region surrounding the hydration products. According to this view, the translational part of the intermediate scattering function (ISF) of the water molecule in a cement paste can be written as follows:

$$F_s(Q,t) = p + (1 - p)F_v(Q,t)\exp[-(t/\tau)^\beta] \qquad (1)$$

where the factor $F_v(Q,t)\exp[-(t/\tau)^\beta]$ is the relaxation function of the glassy water according to the "relaxing cage model" previously given for supercooled water[11] and hydration water in Vycor glass.[21] In fact, in the low Q-range covered in this study, it is reasonable to neglect the rotational contribution coming from the water since it becomes relevant only for Q bigger than 1 $Å^{-1}$.[22] Moreover, $F_v(Q,t)$ is demonstrated to be very close to unity for the time range covered in this experiment so that the ISF for the mobile water reduces only to the exponential term weighed by $(1 - p)$.

The Relaxing-Cage model treats the short time dynamics of glassy water as vibrations of the center-of-mass of a typical water molecule in an ensemble of harmonic wells resulting from the cage effect. The long time dynamic of the water molecule follows the relaxation of the cage and is described by the "α-relaxation" process (the stretched exponential factor) suggested by the "Mode Coupling Theory".[12,13] To take into account the immobile water contribution, we add a constant term p to the ISF. According to this approach, the measured spectral intensity normalized to unity is fitted using the Fourier transform of eq 1 convoluted with the experimental resolution function, $R(\omega)$, to give the following dynamic structure factor:

$$S(Q,\omega) = pR(\omega) + (1 - p)\mathcal{F}\{\exp[-(t/\tau)^\beta]\} \otimes R(\omega) \quad (2)$$

where $\mathcal{F}$ represents the Fourier transform, and $\otimes$ is the convolution operator. In practice, the Fourier transform has been carried out numerically since the analytical form of it does not exist. This dynamical model fits very well the entire set of the spectra collected over 2 days covering an energy transfer range from −1.5 to 0.5 meV. It is worth mentioning that an analytical approach based on the susceptibility function can be successfully applied if the elastic component is not dominant in comparison with the stretched exponential term.[2,6] This statement was proved to be consistent with the numerical analysis.[23]

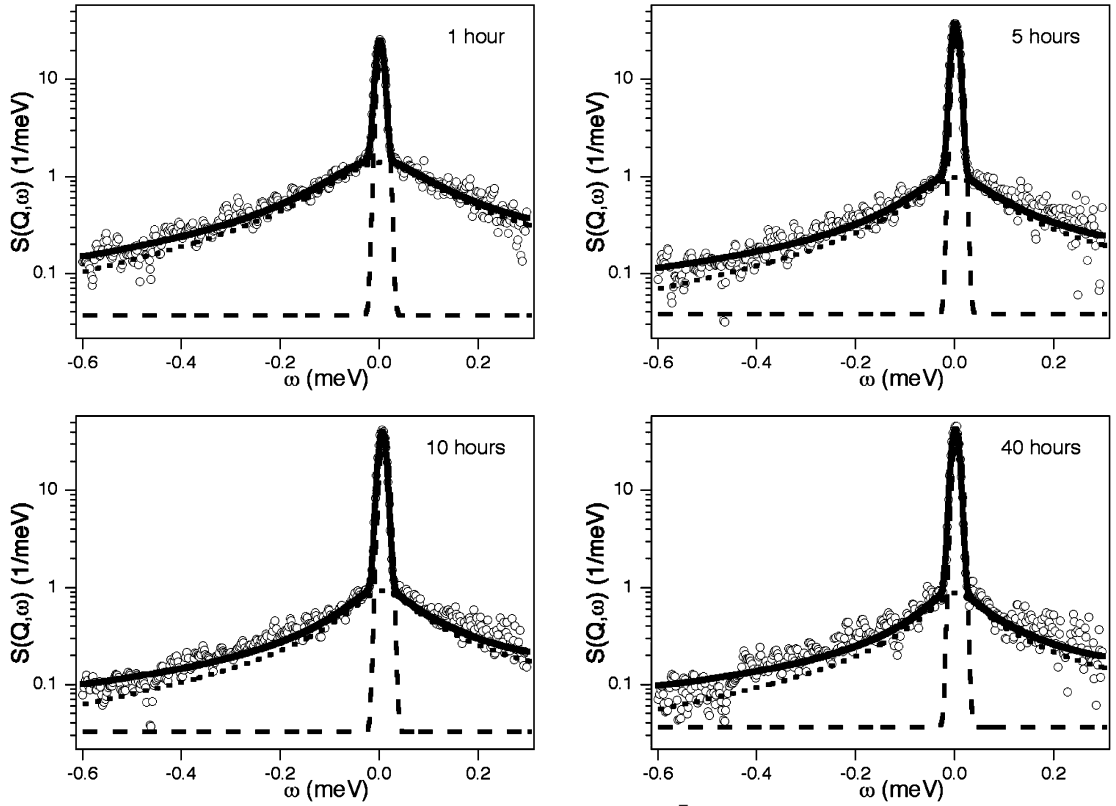

Figure 2. Time evolution of the quasi-elastic incoherent neutron scattering spectra at $\bar{Q} = 1.09 \pm 0.10$ Å^{-1} and $T = 25$ °C in the case of C_3A/H_2O system (reported are 1, 5, 10, and 40 h). The circles represent the normalized experimental spectra, solid lines are the fitted theoretical spectra, the dotted and the dashed lines are the quasi-elastic and the elastic component, respectively, convoluted (see eq 1) with the experimental resolution function, $R(\omega)$. The semilog representation has been used in order to enhance the quasi-elastic part of the spectra.

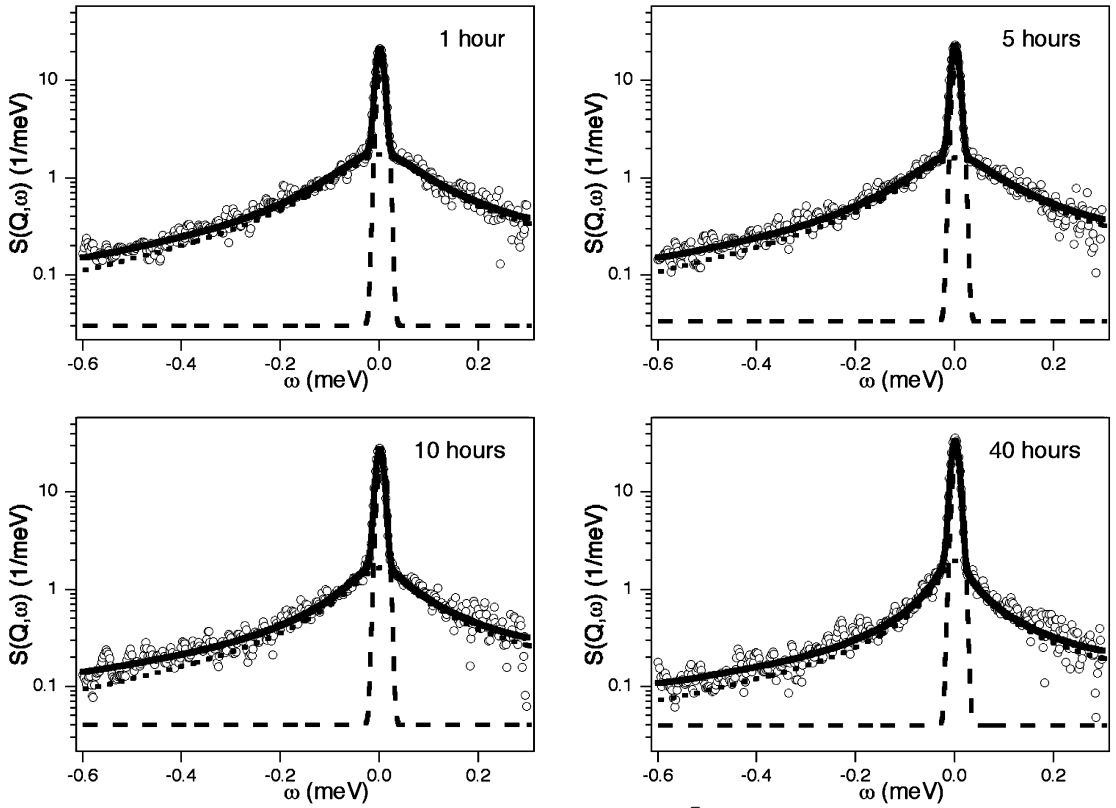

Figure 3. Time evolution of the quasi-elastic incoherent neutron scattering spectra at $\bar{Q} = 1.09 \pm 0.10$ Å^{-1} and $T = 25$ °C in the case of C_4AF/H_2O system (reported are 1, 5, 10 and 40 h). The circles represent the normalized experimental spectra, solid lines are the fitted theoretical spectra, the dotted and the dashed lines are the quasi-elastic and the elastic component respectively convoluted with the experimental resolution function, R(ω).The semilog representation has been used in order to enhance the quasi-elastic part of the spectra.

Figures 2 and 3 show the time evolution of the contributions coming from the hydrogenated species to the QENS spectra at

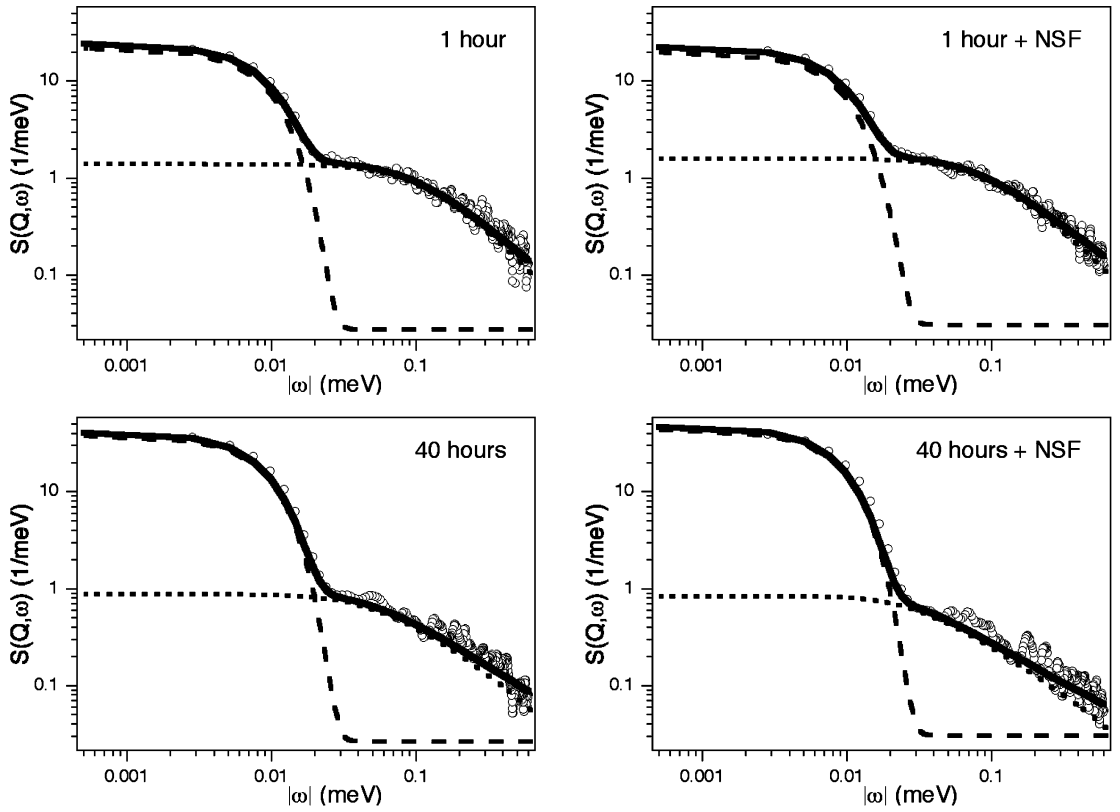

Figure 4. Comparison of the shape evolution of quasi-elastic incoherent neutron scattering spectra in log−log scale at $\bar{Q} = 1.09 \pm 0.10$ Å^{-1} and $T = 25$ °C in the case of C_3A/H_2O system (left panels) and in the presence of an additive (right panels). The circles represent the normalized experimental spectra, solid lines are the fitted theoretical spectra, the dotted and the dashed lines are the quasi-elastic and the elastic components convoluted, respectively, with the experimental resolution function, $R(\omega)$.

$\bar{Q} = 1.09$ Å^{-1} for the two different calcium aluminates, C_3A and C_4AF, within the first 2 days of hydration. The additive case is not reported because the spectra are very similar to the case of C_3A alone being mostly dominated by the elastic peak. In all cases, the elastic peak is already present after 1 h from the mixing time, implying that part of the water has reacted with the powder producing crystalline hydrates. In this crystalline region, the hydrogen translational motion is blocked in the time scale of this *QENS* experiment (2 ps $< t <$ 80 ps) since the area of the elastic peak is constant in the investigated *Q*-range. Moreover, the peak increases as time passes and becomes predominant according to the fact that the water continues to react, becoming part of the aluminate hydrates (immobile fraction). Due to the normalization procedure the area of the elastic peak, *p*, is directly related to the amount of water that has been converted in crystalline hydrates so that, following its time evolution, it is possible to map the kinetics of the hydration reaction directly in situ without perturbing the system (see Figure 5).

A comparison, within the first 40 h, of the quasi-elastic part of the spectra in the case of C_3A without and with NSF is shown in Figure 4. A log−log scale has been used to plot the QENS spectra in order to evidence the effect of the additive on the β exponent (see also Figure 6). In fact, in this plot the slope reached in the linear part ($|\omega| > 0.1$ meV) is directly connected with the stretch exponent β. As we can easily see, the slope is nearly the same after just an hour but its change is more marked after 40 h in the case of the additive NSF, showing that the additive changes the long time relaxation behavior of the mobile water.

Figure 5 shows the change of the immobile water fraction, *p*, as function of time. This parameter is directly connected to

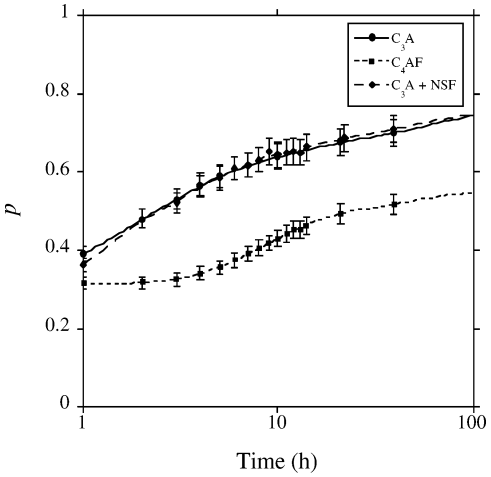

Figure 5. Time evolution of the fraction of immobile water, *p*, at 25 °C in C_3A (full circles), C_4AF (full squares), and C_3A with the NSF additive (full diamonds) that retards the curing process in the case of C_3S.[22]

the reaction degree and permits us to follow the hydration kinetics of the cement paste. As already reported,[1,2] in the case of C_3S and C_2S pastes, *p* is *Q*-independent in the investigated *Q*-range. The two calcium aluminates react differently being the C_4AF phase slower than C_3A phase. The fraction of reacted water is already around 30% for C_4AF and around 40% for C_3A just after 1 h after the mixing time, showing that the induction time is in the time scale of a few minutes, i.e., it is not accessible by using this technique. Moreover, the effect of the NSF on C_3A is negligible on its kinetics evolution so that no effect on the kinetics has been found as in the case of the tri-calcium silicate.[14,15] In fact, in the case of C_3S and C_2S, the

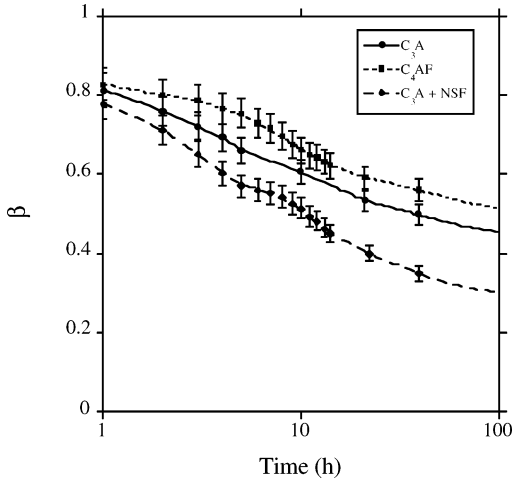

Figure 6. Time evolution of the stretch exponent of the glassy water, β, at 25 °C in C_3A (full circles), C_4AF (full squares), and C_3A with the NSF additive (full diamonds) that retards the curing process in the case of C_3S.

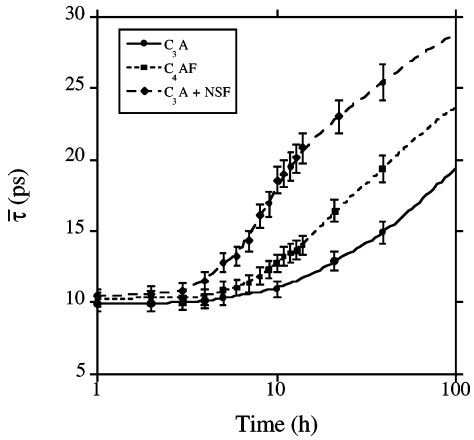

Figure 7. Time evolution of the average relaxation time, $\bar{\tau} = (\tau/\beta)\Gamma(1/\beta)$,[21] at 25 °C in C_3A (full circles), C_4AF (full squares), and C_3A with the NSF additive (full diamonds) that retards the curing process in the case of C_3S. Data obtained using the values at $\bar{Q} = 1.09 \pm 0.10$ Å^{-1}.

addition of superplasticizers does not change the two kinetics laws involved in the hydration processes, (the first according to an Avrami−Erofeyev nucleation and growth law, and the second a three-dimensional diffusion equation), but affects the induction times of the tri-calcium silicate paste and the activation energies related to the nucleation process and growth of the formed nuclei.

Figure 6 shows the time evolution of β in the three cases investigated. The β value decreases as time passes in all cases, showing that the confining properties of the matrix increase in time (i.e., the pore size decreases). In the case of C_3AH_6 the effect is more marked probably because the pores are smaller than in the C_4AF case. The main effect of the additive addition is to decrease even more the final pore size in the aluminate matrix without perturbing the kinetics evolution of the system.

Figure 7 shows the evolution of the average relaxation time, $\bar{\tau}$, at $Q = 1.09$ Å^{-1}, defined as $\bar{\tau} = (\tau/\beta)\Gamma(1/\beta)$.[21] The initial average relaxation time (about 10 ps) is already in all cases more than two times the relaxation time for the bulk water at the same temperature and Q value. As the curing time increases, the average relaxation time increases since the pore size decreases as long as the reaction takes place. NSF addition

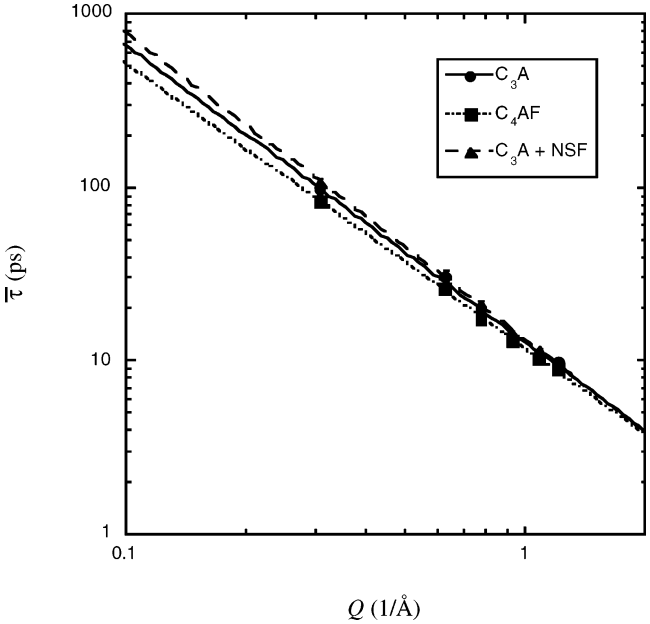

Figure 8. Power law Q-dependence of $\bar{\tau} \propto Q^{-\gamma}$, at 25 °C and averaged over the first 15 h for C_3A (circles), C_4AF (squares), and C_3A with the NSF additive (diamonds). The power law exponent results: $\gamma = 1.71 \pm 0.09$ for C_3A, $\gamma = 1.64 \pm 0.08$ for C_4AF, and $\gamma = 1.78 \pm 0.09$ for C_3A with the NSF additive.

produces a remarkable increase in the relaxation time due to the overall change of the matrix porosity.

In summary, NSF seems to have negligible effect on the p parameter (that is related to the free water index), but it has a dramatic effect on the relaxation parameters of the glassy water, β and $\bar{\tau}$, that is on the "quality" of hydration water. The β value at age of 100 h decreases from 0.45 to 0.3 (the lowest value we ever found in cement pastes by QENS) for C_3A in the presence of NSF. In similar conditions this value for C_3S was 0.7. Interestingly, the corresponding average relaxation time $\bar{\tau}$ increases from 20 ps to nearly 30 ps upon addition of NSF to C_3A supporting the view that NSF increases the water confinement in the growing C_3A matrix.

Finally, Figure 8 shows the power-law dependence $\bar{\tau} \propto Q^{-\gamma}$, in the three cases reported in this paper. The exponent γ is always less than 2, the value associated with the simple diffusion of bulk water at room temperature.[21] The power-law exponent clearly confirms that the mobile water inside the cement matrix presents a relaxation dynamics very far from the bulk water case due to extremely confined environment.

Conclusions

In this paper, we demonstrate that the relaxing cage model earlier developed for C_3S and C_2S[1,2,5] satisfactorily fits all the QENS data in aluminate cement paste as a function of its age. Since the QENS spectra were taken in the low Q region ($Q <$ 1.3 Å^{-1}), only translational motion of water molecules has been considered. The model thus explicitly contains three parameters: p, the fraction of bound water, and β and $\bar{\tau}$, the stretch exponent and the average relaxation time of the glassy water. The QENS measurements reported here account for the late stage of time evolution of these parameters, since the reaction kinetics of the calcium aluminates is very fast compared to that of calcium silicates,[3,17,18] previously investigated.

The maximum p value was about 0.75 and about 0.55 for C_3A C_4AF, respectively, both in agreement with the faster curing

process exhibited by aluminates, while with C_3S we detected a maximum value of about 0.35 at the age of 100 h.

Furthermore the addition of NSF to C_3A does not change the magnitude of the *p* parameter, suggesting that this class of additives does not affect the overall hydration process of alluminates. However, we found that the addition of NSF, while it has no effect on the parameter *p*, it does have a dramatic effect on the relaxation parameters of the glassy water, β and $\bar{\tau}$. Upon the addition of NSF to C_3A, the β value at the age of 100 h decreases from 0.45 to 0.3, the lowest value we ever found in cement pastes. The β value for calcium silicate was 0.7 at 100 h. Likewise the corresponding average relaxation time $\bar{\tau}$ increases from 20 ps to nearly 30 ps upon addition of NSF to C_3A. It can be concluded that the addition of the NSF superplasticizer has the effect of rendering the glassy water even glassier at the late stage of the evolution of the reaction kinetics. These two combined observations indicate that the addition of superplasticizer has the effect of reducing the pore sizes in the final reaction product of the cement paste.

Acknowledgment. The authors gratefully acknowledge CTG-ItalCementi for supplying pure samples of C_3A and C_4AF, and Drs. L. Cassar and S. Biagini for discussion. The authors also express their thanks to J. C. Cook and J. R. D. Copley (NIST Center for Neutron Research, Gaithersburg) for help with the experimental setup and to the NCNR for allocating neutron beam time at DCS spectrometer. Research of S.H.C. was supported by Grant No. DE-FG0290ER45429 from the Material Chemistry Program of the US DOE. Finally, E.F. and P.B. acknowledge CSGI, MURST (Grant PRIN-2001) and CTG-ItalCementi for financial support.

References and Notes

(1) Fratini, E.; Chen, S. H.; Baglioni, P.; Bellissent-Funel, M. C. *J. Phys. Chem. B* **2002**, *106*, 158.

(2) Fratini, E.; Chen, S. H.; Baglioni, P.; Cook, J. C.; Copley, J. R. D. *Phys. Rev. E* **2002**, *65*, 010201.

(3) Taylor, H. W. F. *Cement Chemistry*; Academic Press: London, 1990.

(4) In the well-accepted chemist's notation, letters are used to represent oxides, allowing the chemical formulas of constituent phases to be written in a very concise form: H = H_2O, C = CaO, S = SiO_2, A = Al_2O_3, F = Fe_2O_3, etc. Within this notation the main phases became C_3S, C_2S, C_3A, and C_4AF, respectively, for Ca_3SiO_5, Ca_2SiO_4, $Ca_3Al_2O_6$, and $Ca_4Al_2Fe_2O_{10}$.

(5) Fratini, E.; Chen, S. H.; Baglioni, P.; Bellissent-Funel, M. C. *Phys. Rev. E* **2001**, *64*, 020201.

(6) Fratini, E.; Faraone, A.; Baglioni, P.; Bellissent-Funel, M. C.; Chen, S. H. *Physica A* **2002**, *304*, 1.

(7) Berliner, R.; Popovici, M.; Herwig, K. W.; Berliner, M.; Jennengs, H. M.; Thomas, J. J. *Cem. Concr. Res.* **1998**, *28*, 231.

(8) FitzGerald, S. A.; Neumann, D. A.; Rush, J. J.; Kirkpatrick, R. J.; Cong, X.; Livingston, R. A. *J. Mater. Res.* **1999**, *14*, 1160.

(9) Greener, J.; Peemoeller, H.; Choi, C. H.; Holly, R.; Reardon, E. J.; Hansson, C. M.; Pintar, M. M. *J. Am. Ceram. Soc.* **2000**, *83*, 623.

(10) Magid, L. In *Dynamic Light Scattering. The Methods and Some Applications*; Oxford University Press: Cambridge, 1993; pp 554−593.

(11) Chen, S. H.; Liao, C.; Sciortino, F.; Gallo, P.; Tartaglia, P. *Phys. Rev. E* **1999**, *59*, 6708.

(12) Bengtzelius, U.; Gotze, W.; Sjolander, A. *J. Phys. C* **1984**, *17*, 5915.

(13) Gotze, W.; Sjogren, L. *Rep. Prog. Phys.* **1992**, *55*, 241.

(14) Damasceni, A.; Dei, L.; Fratini, E.; Ridi, F.; Chen, S. H.; Baglioni, P. *J. Phys. Chem. B* **2002**, *106*, 11572.

(15) Ridi, F.; Dei, L.; Fratini, E.; Chen, S. H.; Baglioni, P. *J. Phys. Chem. B* **2003**, *107*, 1056.

(16) Xu, Z.; Viehland, D. *Phys. Rev. Lett.* **1996**, *77*, 952.

(17) Soroka, I. *Portland Cement paste and concrete*; The MacMillan Press LTD: London, 1979.

(18) Bye, G. C. *Portland Cement*, 2nd ed.; Thomas Telford Publishing: London, 1999.

(19) Altorfer, F. B.; Cook, J. C.; Copley, J. R. D. *Mater. Res. Soc. Symp. Proc.* **1995**, *376*, 119.

(20) http://www.ncnr.nist.gov/instruments/dcs/.

(21) Zanotti, J. M.; Bellissent-Funel, M. C.; Chen, S. H. *Phys. Rev. E* **1999**, *59*, 3084.

(22) Faraone, A.; Chen, S. H.; Fratini, E.; Baglioni, P.; Liu, L.; Brown, C. *Phys. Rev. E* **2002**, *65*, 040501.

(23) Baglioni, P.; Fratini, E.; Chen, S. H. *Appl. Phys. A* **2003**, *74*, S1178.